

【DOI】 10.3969 / j.issn.1671-6450.2025.06.018

论著 · 基础

虾青素调控 SLC7A11 减轻非酒精性脂肪性肝病小鼠的铁死亡和自噬水平

柯月, 纪文静, 梁灿灿, 王海昆, 崔旻, 姚萍



基金项目: 国家自然科学基金(82460110); 新疆维吾尔自治区自然科学基金(2021D01C356)

作者单位: 830000 乌鲁木齐, 新疆医科大学第一附属医院消化内科(柯月、王海昆、崔旻、姚萍); 830063 乌鲁木齐, 新疆医科大学第二附属医院消化内科(纪文静、梁灿灿)

通信作者: 姚萍, E-mail: pingyaozh@sina.com

【摘要】目的 探讨虾青素(AST)干预对非酒精性脂肪性肝病(NAFLD)小鼠病理过程影响及其分子机制。**方法** 于2023年6—11月在新疆医科大学动物中心进行实验。通过高脂饮食建立NAFLD小鼠模型,随机分为NAFLD组、NAFLD+铁死亡激活剂(Erastin)组、NAFLD+AST组,每组10只,并行相应干预,另取10只正常小鼠作空白对照组。利用免疫组化检测肝组织中溶质载体家族7成员11(SLC7A11)蛋白表达;HE染色观察肝组织炎症反应和结构变化;ELISA检测脂代谢指标[总胆固醇(TC)、三酰甘油(TG)、低密度脂蛋白胆固醇(LDL-C)]、氧化应激[谷胱甘肽(GSH)、活性氧(ROS)、丙二醛(MDA)、肿瘤坏死因子 α (TNF- α)]、炎症因子[白介素-6(IL-6)]水平;RT-qPCR及Western blot检测铁死亡[谷胱甘肽过氧化物酶4(GPX4)、血红素加氧酶1(HMOX1)、SLC7A11]、自噬(LC3B、p62)相关指标mRNA及蛋白表达。**结果** 免疫组化显示,与空白对照组比较,NAFLD组SLC7A11蛋白表达下降($P < 0.05$);与NAFLD组比较,NAFLD+Erastin组SLC7A11蛋白表达下降,NAFLD+AST组SLC7A11蛋白表达升高($P < 0.05$);与NAFLD+AST组比较,NAFLD+Erastin组的SLC7A11蛋白表达水平降低($P < 0.05$)。HE染色结果表明,与空白对照组比较,NAFLD组的肝组织中炎症反应表现加重;与NAFLD组比较,NAFLD+Erastin组的炎症反应进一步加重,NAFLD+AST组的炎症反应则有所减轻;NAFLD+AST组的炎症反应较NAFLD+Erastin组明显减轻。与空白对照组比较,NAFLD组小鼠血清TG、TC、LDL-C水平均显著升高($P < 0.05$);与NAFLD组比较,NAFLD+Erastin组TG、TC、LDL-C水平均升高,NAFLD+AST组TG、TC、LDL-C水平均降低($P < 0.05$);NAFLD+Erastin组的TG、TC、LDL-C水平较NAFLD+AST组明显升高($P < 0.05$)。与空白对照组比较,NAFLD组血清GSH水平降低,ROS、MDA、TNF- α 、IL-6水平升高($P < 0.05$);与NAFLD组比较,NAFLD+Erastin组GSH降低,ROS、MDA、TNF- α 、IL-6水平升高($P < 0.05$),NAFLD+AST组GSH水平升高,ROS、MDA、TNF- α 、IL-6水平降低($P < 0.05$);与NAFLD+Erastin组比较,NAFLD+AST组GSH水平升高,ROS、MDA、TNF- α 、IL-6水平降低($P < 0.05$)。与空白对照组比较,NAFLD组肝组织中GPX4、HMOX1、SLC7A11、p62 mRNA及蛋白表达下调,LC3B mRNA及蛋白表达上调($P < 0.05$);与NAFLD组比较,NAFLD+Erastin组GPX4、HMOX1、SLC7A11、p62 mRNA及蛋白表达均降低,LC3B mRNA及蛋白表达升高($P < 0.05$),NAFLD+AST组GPX4、HMOX1、SLC7A11、p62 mRNA及蛋白表达均升高,LC3B mRNA及蛋白表达降低($P < 0.05$);与NAFLD+Erastin组比较,NAFLD+AST组GPX4、HMOX1、SLC7A11、p62 mRNA及蛋白表达升高,LC3B mRNA及蛋白表达降低($P < 0.05$)。**结论** AST干预可能通过上调SLC7A11的表达调控铁死亡与自噬途径,从而改善NAFLD小鼠的肝组织病理变化,降低氧化应激及炎症反应水平。

【关键词】 非酒精性脂肪性肝病;虾青素;溶质载体家族7成员11;铁死亡;自噬;小鼠**【中图分类号】** R575.5 **【文献标识码】** A**Astaxanthin regulates SLC7A11 to attenuate ferroptosis and autophagy levels in mice with non-alcoholic fatty liver disease**

Ke Yue*, Ji Wenjing, Liang Cancan, Wang Haikun, Cui Min, Yao Ping.* Department of Gastroenterology, the First Affiliated Hospital of Xinjiang Medical University, Xinjiang, Urumqi 830000, China

Funding program: National Natural Science Foundation of China (82460110); the Natural Science Foundation of Xinjiang Uygur Autonomous Region (2021D01C356)

Corresponding author: Yao Ping, E-mail: pingyaozh@sina.com

【Abstract】 Objective To investigate the effect of astaxanthin (AST) intervention on the pathological process of mice

with non-alcoholic fatty liver disease (NAFLD) and its molecular mechanism. **Methods** This study was conducted from June to November 2023 at the Animal Center of Xinjiang Medical University. A NAFLD mouse model was established using a high-fat diet, and mice were randomly divided into four groups: Control group, NAFLD group, NAFLD+Erastin group and NAFLD+AST group. Immunohistochemistry was used to detect the protein expression of SLC7A11 in liver tissues. Hematoxylin-eosin (HE) staining was performed to observe inflammatory responses and structural changes in liver tissues. Enzyme-linked immunosorbent assay (ELISA) was conducted to measure the levels of blood lipids and inflammatory factors. Additionally, quantitative real-time polymerase chain reaction (RT-qPCR) and Western blot analyses were used to assess the expression levels of ferroptosis - related molecules (GPX4, HMOX1, SLC7A11) and autophagy - related molecules (LC3, p62). **Results** Immunohistochemistry showed that, compared with the blank control group, the expression of SLC7A11 protein in the NAFLD group decreased ($P < 0.05$). Compared with the NAFLD group, the expression of SLC7A11 protein in the NAFLD+Erastin group decreased ($P < 0.05$), while the expression of SLC7A11 protein in the NAFLD+AST group increased ($P < 0.05$). Compared with the NAFLD+AST group, the expression level of SLC7A11 protein in the NAFLD+Erastin group was lower ($P < 0.05$). The results of HE staining indicated that, compared with the blank control group, the inflammatory response in the liver tissue of the NAFLD group was exacerbated. When compared with the NAFLD group, the inflammatory response in the NAFLD+Erastin group was further aggravated, while that in the NAFLD+AST group was alleviated. AST can effectively reduce the inflammatory response in the liver tissue. The inflammatory response in the NAFLD+AST group was significantly milder than that in the NAFLD+Erastin group. The detection of serum indicators showed that, compared with the blank control group, the levels of triglyceride (TG), total cholesterol (TC), and low-density lipoprotein Cholesterol (LDL-C) in the serum of mice in the NAFLD group were significantly increased ($P < 0.05$). Compared with the NAFLD group, the levels of TG, TC, and LDL-C in the NAFLD+Erastin group were all increased ($P < 0.05$), while the levels of TG, TC, and LDL-C in the NAFLD+AST group were all decreased ($P < 0.05$). The levels of TG, TC, and LDL-C in the NAFLD+Erastin group were significantly higher than those in the NAFLD+AST group ($P < 0.05$). Compared with the blank control group, the level of glutathione (GSH) in the NAFLD group was decreased ($P < 0.05$), while the levels of reactive oxygen species (ROS), malondialdehyde (MDA), tumor necrosis factor- α (TNF- α), and interleukin-6 (IL-6) were increased ($P < 0.05$). Compared with the NAFLD group, the level of GSH in the NAFLD+AST group was increased ($P < 0.05$), and the levels of ROS, MDA, TNF- α , and IL-6 were decreased ($P < 0.05$). In the NAFLD+Erastin group, except that the level of GSH was decreased ($P < 0.05$), the levels of ROS, MDA, TNF- α , and IL-6 were all increased ($P < 0.05$). Compared with the NAFLD+Erastin group, the level of GSH in the NAFLD+AST group was significantly increased ($P < 0.05$), and the levels of ROS, MDA, TNF- α , and IL-6 were decreased to some extent ($P < 0.05$). Molecular - level analysis revealed that qRT - PCR results showed that, compared with the blank control group, the expressions of GPX4, HMOX1, p62, and SLC7A11 in the NAFLD group were downregulated ($P < 0.05$), while the expression of LC3B was upregulated ($P < 0.05$). Compared with the NAFLD group, the expressions of GPX4, HMOX1, SLC7A11, and p62 in the NAFLD+Erastin group were all decreased ($P < 0.05$), and the level of LC3B was increased ($P < 0.05$). In the NAFLD+AST group, the level of LC3B was decreased ($P < 0.05$), and the expressions of GPX4, HMOX1, SLC7A11, and p62 were all increased ($P < 0.05$). The expression levels of GPX4, HMOX1, SLC7A11, and p62 in the NAFLD+AST group were higher than those in the NAFLD+Erastin group ($P < 0.05$), while the expression of LC3B was decreased ($P < 0.05$). The results of Western Blot showed that compared with the blank control group, the expression of LC3B in the NAFLD group was upregulated ($P < 0.05$), and the protein expressions of GPX4, HMOX1, p62, and SLC7A11 were all downregulated ($P < 0.05$). Compared with the NAFLD group, the expression of LC3B in the NAFLD+Erastin group was upregulated ($P < 0.05$), and the expressions of GPX4, HMOX1, SLC7A11, and p62 were downregulated ($P < 0.05$). In the NAFLD+AST group, the expression of LC3B was downregulated ($P < 0.05$), and the expressions of GPX4, HMOX1, SLC7A11, and p62 were all upregulated ($P < 0.05$). The expression of LC3B in the NAFLD+Erastin group was lower than that in the NAFLD+AST group ($P < 0.05$), and the expressions of GPX4, HMOX1, SLC7A11, and p62 were all increased ($P < 0.05$). **Conclusion** AST intervention may regulate the ferroptosis and autophagy pathways by upregulating the expression of SLC7A11, thereby improving the pathological changes of liver tissues in NAFLD mice, reducing the levels of oxidative stress and inflammatory response, and providing potential new targets and innovative ideas for the treatment of NAFLD.

【Key words】 Non-alcoholic fatty liver disease; Astaxanthin; SLC7A11; Ferroptosis; Autophagy; Mice

非酒精性脂肪性肝病 (nonalcoholic fatty liver disease, NAFLD) 作为全球肝病的主要原因之一, 2021 年全球汇总患病率为 32.4%, 预计到 2030 年将进一步增加^[1]。NAFLD 与肥胖、糖尿病等代谢疾病密切相关, 涉及脂质代谢紊乱、氧化应激、炎症反应及细胞信号通路异常, 可能发展为肝硬化或肝癌, 严重威胁患者健康^[2-3]。尽管其病理机制复杂, 调控上述过程的关键分子仍有待深入探索。溶质载体家族 7 成员 11 (solute carrier family 7 member 11, SLC7A11) 负责输入半胱氨酸和输出谷氨酸, 通过调节氧化、减少炎症反应和纤维化起到保护作用^[4]。然而, 目前关于 SLC7A11 在 NAFLD 中的表达和功能的研究较少。虾青素 (astaxanthin, AST) 具有抗氧化活性, 在心血管疾病、糖尿病和癌症动物模型中显示出治疗潜力, 可清除活性氧自由基, 减轻氧化应激损伤, 并可能改善肝脏脂质代谢和炎症反应, 但其在 NAFLD 中对 SLC7A11 及相关细胞通路的调控机制尚不明确^[5-6]。铁死亡涉及脂质的铁依赖性过氧化, 与 NAFLD 的发病机制密切相关^[7]。此外, 自噬可以维持非实质细胞类型的稳态和功能, 从而抑制肝脏炎症反应和纤维化, 减缓 NAFLD 的进展^[8]。本研究通过建立 NAFLD 小鼠模型, 观察 AST 干预对肝脏组织形态、脂质代谢、氧化应激、炎症因子、铁死亡和自噬的影响, 旨在揭示 AST 治疗 NAFLD 的分子机制, 为临床提供新理论依据和潜在靶点, 报道如下。

1 材料与方 法

1.1 材料 (1) 动物: C57BL/6J 品系小鼠 40 只, 雄性, 体质量 18~20 g, 6~8 周龄, 购自新疆医科大学动物中心 [许可证号 SYXK (新) 2023-0004]。本研究严格遵循国际实验动物伦理学要求, 并已获得新疆医科大学第一附属医院医学伦理委员会的审批 (K202309-11)。(2) 药物与试剂: AST (上海源叶生物科技有限公司, 货号: 472-61-7); 二甲亚砜 (DMSO, 上海碧云天生物技术有限公司, 货号: ST038-500ml); 铁死亡诱导剂 (Erastin, 美国 MCE 公司, 货号: 571203-78-6); 血脂、炎症因子测定试剂盒 (南京建成生物工程研究所有限公司); 活性氧 (ROS) 测定试剂盒 (上海艾博抗贸易有限公司, 货号: ab279910); 总 RNA 提取试剂 (TRIzol 试剂, 美国 Invitrogen 公司, 货号: 15596018CN); 逆转录试剂盒 (日本 Takara, 货号: RR430S); TB Green Premix Ex Taq II (日本 Takara, 货号: RR820A); BeyoBCA 蛋白浓度快速测定试剂盒 (上海碧云天生物技术有限公司, 货号: P0398S); 抗体测定试剂盒 (武汉爱博泰克

公司)。(3) 仪器设备: Leica RM2245 石蜡切片机 (德国徕卡显微系统有限公司), 正置显微镜 (日本奥林巴斯公司), ABI 7500 Fast 实时荧光定量聚合酶链式反应仪 (赛默飞世尔科技公司), Amersham Imager 600 化学发光成像仪 (美国 GE 公司)。

1.2 NAFLD 小鼠模型的构建与分组 于 2023 年 6—11 月在新疆医科大学动物中心进行实验。选取 C57BL/6J 品系雄性小鼠 40 只, 适应性饲养 1 周 (温度 22~25℃、湿度为 40%~60%, 12 h 光照/12 h 黑暗循环) 后开始建模。将小鼠随机分为 4 组: 空白对照组 (正常小鼠给予 DMSO 干预)、NAFLD 组 (NAFLD 小鼠给予 DMSO 干预)、NAFLD+Erastin 组 (NAFLD 小鼠给予 Erastin 干预)、NAFLD+AST 组 (NAFLD 小鼠给予 AST 干预), 每组 10 只。除空白对照组给予普通饲料喂养外, 其余小鼠均给予高脂饲料 (饲料配方: 88% 基础饲料、10% 猪油、2% 胆固醇) 喂养, 持续喂养 12 周, 诱导建立 NAFLD 小鼠模型 (成功条件: 造模 12 周后处死小鼠, 取肝组织经 HE 染色观察其病理学特征, NAFLD 组可见肝细胞内脂滴沉积, 部分脂滴形成空泡, 肝细胞体积增大)。造模期间每周监测小鼠体质量、饮食量等。干预措施: 从实验开始至第 12 周, NAFLD+Erastin 组小鼠每周 3 次腹腔注射 Erastin 10 mmol/kg, NAFLD+AST 组小鼠每日 1 次灌胃给予 AST 30 mg/kg。

1.3 观测指标与方法

1.3.1 免疫组化检测肝组织 SLC7A11 表达水平: 取小鼠肝脏组织, 用 4% 多聚甲醛固定 24 h 后进行脱水、透明、浸蜡、包埋, 切片厚度约 4 μm。将切片脱蜡至水后采用高压修复法进行抗原修复, 用 3% H₂O₂ 室温孵育 10 min 以阻断内源性过氧化物酶活性, 正常山羊血清封闭 30 min。加入一抗 (SLC7A11 抗体, 1:200 稀释), 4℃ 孵育过夜。用磷酸盐缓冲盐水 (PBS) 洗片 3 次, 每次 5 min, 加入二抗 (1:200 稀释), 室温孵育 30 min。再次用 PBS 洗片后, 使用二氨基联苯胺 (DAB) 显色试剂盒显色, 苏木精复染细胞核, 梯度酒精脱水, 二甲苯透明, 中性树胶封片。在显微镜下观察并采集图像。

1.3.2 HE 染色观察肝组织炎症反应和结构变化: 将上述小鼠肝脏组织切片经二甲苯脱蜡, 梯度酒精水化, 用苏木精染液染色 5 min, 水洗后用 1% 盐酸酒精分化 3~5 s, 再用伊红染液染色 2 min。脱水、透明、封片后在显微镜下观察肝组织的病理形态学变化, 包括肝细胞脂肪变性程度、炎症细胞浸润情况以及肝小叶结构完整性等。

1.3.3 ELISA 检测血清脂代谢、氧化应激、炎症因子水

平:将小鼠血样在室温静置 2 h 后,离心留取血清待测。使用 ELISA 试剂盒(南京建成)分别检测总胆固醇(TC)、三酰甘油(TG)、低密度脂蛋白胆固醇(LDL-C)、谷胱甘肽(GSH)、ROS、丙二醛(MDA)、肿瘤坏死因子 α (TNF- α)、白介素-6(IL-6)水平。加样后,在 37℃ 孵育 2 h,洗板 3 次,每次浸泡 1~2 min,拍干后加入酶标抗体,再在 37℃ 孵育 1 h,洗板后加入底物溶液,避光显色 15 min,加入终止液。在酶标仪上测定各孔在特定波长下的吸光度值,根据标准曲线计算各指标的含量。

1.3.4 RT-qPCR 检测肝组织中铁死亡、自噬相关指标 mRNA 表达:铁死亡相关指标包括谷胱甘肽过氧化物酶 4(GPX4)、血红素加氧酶 1(HMOX1)、SLC7A11,自噬相关指标包括 LC3B、p62。采用 TRIzol 试剂提取小鼠肝组织的总 RNA,用紫外分光光度计测定 RNA 的浓度和纯度,A260/A280 在 1.8~2.0 之间为合格。取 RNA 1 μ g 进行逆转录反应,使用逆转录试剂盒(Takara)合成 cDNA。逆转录反应在 37℃ 孵育 60 min,85℃ 加热 5 min 后终止反应。qPCR 反应体系 20 μ l:SYBR Green PCR Master Mix(Takara)10 μ l,上下游引物各 0.5 μ l,cDNA 模板 2 μ l,ddH₂O 7 μ l。qPCR 扩增条件:预变性 95℃ 5 min、95℃ 15 s、退火 60℃ 30 s、延伸 72℃ 30 s,共计 40 个循环。引物序列:GPX4 上游引物 5'-GCCAAAGTCCTAGGAAACGC-3',下游引物 5'-CCGGGTGAAAGGTTTCAGGA-3';HMOX1 上游引物 5'-CCTCACAGATGGCGTCACTT-3',下游引物 5'-TGGGGGCCAGTATTGCATTT-3';SLC7A11 上游引物 5'-AATACGGAGCCTTCCACGAG-3',下游引物 5'-CTC-CAGGGGCAGTCAGTTAG-3';p62 上游引物 5'-GGAC-CCATCTACAGAGGCTG-3',下游引物 5'-ATCACAATG-GTGGAGGGTGC-3';LC3B 上游引物 5'-GGGACCCTAAC-CCCATAGGA-3',下游引物 5'-GGCACCAGGAACCTG-GTCTT-3'; β -actin 上游引物 5'-CTTCGCGGGCGACGAT-3',下游引物 5'-CCACATAGGAATCCTTCTGACC-3'。以 β -actin 为内参基因,采用 2^{- $\Delta\Delta$ Ct} 法计算目的基因相对表达量。

1.3.5 Western blot 检测肝组织中铁死亡、自噬相关指标蛋白水平:将小鼠肝组织按 1:10 加入含有蛋白酶抑制剂和磷酸酶抑制剂的 RIPA 裂解液中提取总蛋白,使用 BCA 蛋白定量试剂盒(Biosharp)测定蛋白浓度。取 30 μ g 蛋白样品进行 SDS-PAGE 电泳(浓缩胶浓度为 5%,分离胶浓度为 12%)分离。随后将蛋白转移至聚偏氟乙烯(PVDF)膜上。用 5%脱脂奶粉室温封闭膜 1 h,加入按 1:1 000 比例稀释的一抗工作液

(GPX4、HMOX1、SLC7A11、LC3B、p62 及内参蛋白 β -actin 的抗体),4℃ 孵育过夜。次日用 TBST 洗膜 3 次,每次 10 min,加入按 1:5 000 比例稀释的二抗工作液,室温孵育 1 h,再次用 TBST 洗膜后。用 ECL 化学发光试剂(索莱宝)显色,在凝胶成像系统中曝光并采集图像,用 ImageJ 软件分析目的蛋白条带的灰度值,以 β -actin 为内参,计算蛋白的相对表达量。

1.4 统计学方法 采用 Graphpad Prism 4.0 软件对数据进行统计分析。正态分布计量资料以均值 \pm 标准差表示,2 组间比较采用 *t* 检验,多组间比较采用单因素方差分析(ANOVA);计数资料以频数/构成比(%)表示,组间比较采用 χ^2 检验。*P*<0.05 为差异有统计学意义。

2 结果

2.1 各组小鼠肝组织 SLC7A11 蛋白水平比较 与空白对照组比较,NAFLD 组 SLC7A11 蛋白表达下降(*t*/*P*=6.225/0.003);与 NAFLD 组比较,NAFLD+Erastin 组 SLC7A11 蛋白表达下降(*t*/*P*=2.852/0.046),NAFLD+AST 组 SLC7A11 蛋白表达升高(*t*/*P*=3.111/0.036);与 NAFLD+Erastin 组比较,NAFLD+AST 组 SLC7A11 蛋白表达水平升高(*t*/*P*=5.595/0.005),见图 1、表 1。

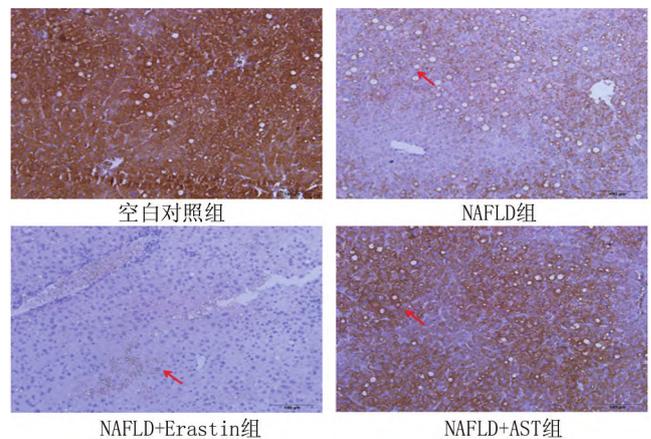


图 1 各组小鼠肝组织 SLC7A11 水平比较(免疫组化染色,×100)

Fig.1 Comparison of SLC7A11 levels in liver tissues of mice in different groups (immunohistochemistry staining, × 100)

2.2 各组小鼠肝组织炎症反应与结构变化 与空白对照组比较,NAFLD 组肝组织中炎症反应表现严重;与 NAFLD 组比较,NAFLD+Erastin 组的炎症反应进一步加重,NAFLD+AST 组的炎症反应则有所减轻;NAFLD+AST 组的炎症反应较 NAFLD+Erastin 组明显减轻,见图 2。

表 1 免疫组化检测各组小鼠肝组织 SLC7A11 蛋白水平 ($\bar{x}\pm s$)

Tab.1 Immunohistochemical detection of SLC7A11 protein levels in liver tissues of mice in each group

组别	n	SLC7A11
空白对照组	10	0.517±0.105
NAFLD 组	10	0.114±0.039 ^a
NAFLD+Erastin 组	10	0.037±0.025 ^b
NAFLD+AST 组	10	0.238±0.057 ^{bc}
F/P 值		32.352/<0.001

注:与空白对照组比较,^a $P<0.05$;与 NAFLD 组比较,^b $P<0.05$;与 NAFLD+Erastin 组比较,^c $P<0.05$ 。

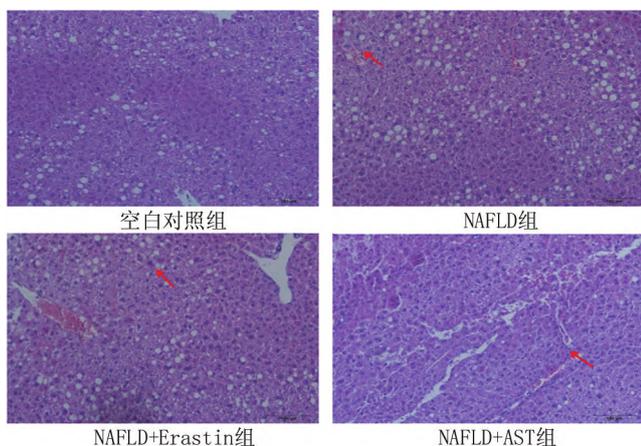


图 2 各组小鼠肝组织炎症反应与结构变化比较(HE 染色, × 100)

Fig.2 Comparison of inflammatory response and structural changes in liver tissue of mice in each group (HE staining, × 100)

2.3 各组小鼠血清脂质代谢指标比较 与空白对照组比较,NAFLD 组小鼠血清 TG、TC、LDL-C 水平均显著升高($t/P=13.087/<0.001, 7.813/0.001, 119.520/<0.001$);与 NAFLD 组比较,NAFLD+Erastin 组 TG、TC、LDL-C 水平均升高($t/P=8.176/<0.001, 4.649/0.010, 7.914/<0.001$), NAFLD+AST 组 TG、TC、LDL-C 水平均降低($t/P=4.747/0.001, 4.073/0.015, 26.863/<0.001$);

NAFLD+AST 组 TG、TC、LDL-C 水平均低于 NAFLD+Erastin 组($t/P=16.438/<0.001, 8.104/0.001, 10.049/<0.001$),见表 2。

表 2 各组小鼠血清 TG、TC、LDL-C 水平比较 ($\bar{x}\pm s, \text{mmol/L}$)

Tab.2 Comparison of serum TG, TC, and LDL-C levels among different groups of mice

组别	n	TG	TC	LDL-C
空白对照组	10	0.545±0.023	1.425±0.047	0.761±0.016
NAFLD 组	10	0.983±0.071 ^a	2.290±0.186 ^a	1.684±0.006 ^a
NAFLD+Erastin 组	10	1.272±0.034 ^b	3.172±0.271 ^b	2.469±0.222 ^b
NAFLD+AST 组	10	0.791±0.056 ^{bc}	1.737±0.145 ^{bc}	1.460±0.045 ^{bc}
F/P 值		190.889/<0.001	53.781/<0.001	198.534/<0.001

注:与空白对照组比较,^a $P<0.05$;与 NAFLD 组比较,^b $P<0.05$;与 NAFLD+Erastin 组比较,^c $P<0.05$ 。

2.4 各组小鼠血清氧化应激、炎症因子水平比较 与空白对照组比较,NAFLD 组 GSH 水平降低,ROS、MDA、TNF- α 、IL-6 水平升高($t/P=10.114/<0.001, 6.642/<0.001, 33.771/<0.001, 20.481/<0.001, 8.998/<0.001$);与 NAFLD 组比较,NAFLD+Erastin 组 GSH 水平降低,ROS、MDA、TNF- α 、IL-6 水平升高($t/P=10.523/<0.001, 4.365/0.002, 7.222/<0.001, 9.659/0.031, 2.520/0.036$), NAFLD+AST 组 GSH 水平升高,ROS、MDA、TNF- α 、IL-6 水平降低($t/P=10.817/<0.001, 2.805/0.023, 11.430/<0.001, 2.618/0.031, 4.762/0.001$);与 NAFLD+Erastin 组比较,NAFLD+AST 组 GSH 水平升高,ROS、MDA、TNF- α 、IL-6 水平降低($t/P=33.715/<0.001, 13.032/<0.001, 15.512/<0.001, 6.281/<0.001, 4.874/0.001$),见表 3。

2.5 各组小鼠肝组织铁死亡相关基因、自噬标志物 mRNA 及蛋白表达比较 与空白对照组比较,NAFLD 组 GPX4、HMOX1、SLC7A11、p62 mRNA 表达下调,LC3B mRNA 表达上调($t/P=14.896/<0.001, 13.147/<0.001, 9.392/<0.001, 10.179/<0.001, 15.184/<0.001$);与 NAFLD 组比较,NAFLD+Erastin 组 GPX4、HMOX1、

表 3 各组小鼠血清 GSH、ROS、MDA、TNF- α 、IL-6 水平比较 ($\bar{x}\pm s$)

Tab.3 Comparison of serum GSH, ROS, MDA, TNF - α , and IL-6 levels among different groups of mice

组别	n	GSH (ng/L)	ROS ($\mu\text{g/L}$)	MDA ($\mu\text{g/L}$)	TNF- α ($\mu\text{g/L}$)	IL-6 (ng/L)
空白对照组	10	1.392±0.200	1.254±0.033	1.051±0.026	1.579±0.055	1.500±0.227
NAFLD 组	10	0.472±0.035 ^a	1.717±0.152 ^a	1.943±0.053 ^a	2.195±0.038 ^a	2.415±0.008 ^a
NAFLD+Erastin 组	10	0.300±0.010 ^b	2.030±0.051 ^b	2.272±0.087 ^b	2.682±0.106 ^b	2.622±0.184 ^b
NAFLD+AST 组	10	0.673±0.022 ^{bc}	1.504±0.074 ^{bc}	1.451±0.080 ^{bc}	1.882±0.264 ^{bc}	2.122±0.137 ^{bc}
F/P 值		109.787/<0.001	66.829/<0.001	330.367/<0.001	51.834/<0.001	45.778/<0.001

注:与空白对照组比较,^a $P<0.05$;与 NAFLD 组比较,^b $P<0.05$;与 NAFLD+Erastin 组比较,^c $P<0.05$ 。

SLC7A11、p62 mRNA 表达均降低,LC3B mRNA 表达水平升高 ($t/P = 5.900/0.004, 9.314/<0.001, 12.049/<0.001, 3.830/0.019, 6.922/0.002$), NAFLD + AST 组 GPX4、HMOX1、SLC7A11、p62 mRNA 表达升高,LC3B mRNA 表达降低 ($t/P = 6.980/0.002, 3.870/0.018, 4.263/0.013, 3.702/0.021, 5.081/0.007$); 与 NAFLD + Erastin 组比较, NAFLD + AST 组 GPX4、HMOX1、SLC7A11、p62 mRNA 表达水平升高,LC3B mRNA 表达水平降低 ($t/P = 9.592/<0.001, 6.757/0.003, 11.494/<0.001, 7.840/0.001, 13.782/<0.001$), 见表 4。

与空白对照组比较, NAFLD 组 GPX4、HMOX1、SLC7A11、p62 蛋白表达下调,LC3B 蛋白表达上调 ($t/P = 7.693/0.002, 23.170/<0.001, 9.587/<0.001, 11.353/<0.001, 21.355/<0.001$); 与 NAFLD 组比较, NAFLD+Erastin 组 GPX4、HMOX1、SLC7A11、p62 蛋白表达下调,LC3B 蛋白表达上调 ($t/P = 4.169/0.014, 16.906/<0.001, 6.364/0.003, 10.635/<0.001, 3.559/0.024$), NAFLD + AST 组 GPX4、HMOX1、SLC7A11、p62 蛋白表达上调,LC3B 蛋白表达下调 ($t/P = 3.922/0.017, 11.236/<0.001, 4.932/0.008, 3.342/0.029, 5.234/0.006$); 与 NAFLD + Erastin 组比较, NAFLD + AST 组 GPX4、HMOX1、SLC7A11、p62 蛋白表达升高,LC3B 蛋白表达降低 ($t/P = 11.255/<0.001, 47.450/<0.001, 25.612/<0.001, 33.910/<0.001, 10.622/<0.001$), 见表 5。

3 讨论

本研究显示,AST 通过激活抗氧化和抗炎机制,以

及可能通过促进 SLC7A11 表达减轻铁死亡,进而缓解 NAFLD 小鼠模型中的肝脏炎症反应和氧化损伤。

首先,SLC7A11 在 NAFLD 小鼠模型中的表达上调显著减轻了肝脏的炎症反应。SLC7A11 作为一个重要的氨基酸转运蛋白,已知它在细胞的氧化还原平衡中发挥着关键作用^[4, 9]。在 NAFLD 中,氧化应激是推动肝脏病理进展的核心因素,SLC7A11 的表达上调可能通过增强细胞内的抗氧化能力,调节脂质代谢,减少脂肪沉积,从而缓解肝脏的氧化损伤和炎症反应,这一结果与以往研究中 SLC7A11 对抗氧化损伤的作用相吻合^[10-11]。本研究进一步表明,SLC7A11 在 NAFLD 发展过程中可能通过调节自噬和铁死亡的途径发挥作用。

此外,AST 作为具有抗氧化活性的天然化合物,可通过激活特定的转录因子或信号通路来影响细胞的氧化还原稳态和代谢功能^[12]。AST 干预能够显著减少肝脏炎症反应,这一结果与既往研究中 AST 在肝脏疾病模型中的抗炎作用相吻合^[13-14]。本研究进一步揭示,AST 可能通过调控 SLC7A11 的表达增强细胞抗氧化能力,进而抑制脂质过氧化和铁死亡。同时,AST 介导的 SLC7A11 上调也有效调控了异常激活的自噬通路,表现为 LC3B 水平降低、p62 水平恢复,进而减轻自噬异常激活对肝细胞造成的损伤。这一发现进一步明确了 AST 通过 SLC7A11 表达调控 NAFLD 中铁死亡和自噬异常的具体机制。这一点与其他文献中 AST 的作用机制略有不同,提供了新的药物相互作用机制的思路。

表 4 各组小鼠肝组织 GPX4、HMOX1、SLC7A11、LC3B、p62 mRNA 水平比较 ($\bar{x}\pm s$)

Tab.4 Comparison of GPX4, HMOX1, SLC7A11, LC3B, and p62 mRNA levels in liver tissues of mice in each group

组别	n	GPX4	HMOX1	SLC7A11	LC3B	p62
空白对照组	10	1.001±0.028	1.027±0.046	0.994±0.040	0.991±0.017	1.007±0.017
NAFLD 组	10	0.728±0.015 ^a	0.640±0.021 ^a	0.754±0.008 ^a	1.470±0.052 ^a	0.690±0.056 ^a
NAFLD+Erastin 组	10	0.571±0.044 ^b	0.522±0.007 ^b	0.519±0.033 ^b	1.709±0.287 ^b	0.506±0.061 ^b
NAFLD+AST 组	10	0.864±0.030 ^{bc}	0.811±0.074 ^{bc}	0.846±0.037 ^{bc}	1.261±0.048 ^{bc}	0.836±0.040 ^{bc}
F/P 值		107.201/<0.001	71.308/<0.001	116.120/<0.001	182.037/<0.001	62.329/<0.001

注:与空白对照组比较,^a $P<0.05$;与 NAFLD 组比较,^b $P<0.05$;与 NAFLD+Erastin 组比较,^c $P<0.05$ 。

表 5 各组小鼠肝组织 GPX4、HMOX1、SLC7A11、LC3B、p62 蛋白水平比较 ($\bar{x}\pm s$)

Tab.5 Comparison of GPX4, HMOX1, SLC7A11, LC3B, and p62 protein levels in liver tissues of mice in each group

组别	n	GPX4	HMOX1	SLC7A11	LC3B	p62
空白对照组	10	1.000±0.030	1.000±0.015	1.000±0.014	1.000±0.039	1.000±0.029
NAFLD 组	10	0.762±0.044 ^a	0.657±0.021 ^a	0.800±0.027 ^a	1.834±0.055 ^a	0.730±0.039 ^a
NAFLD+Erastin 组	10	0.633±0.031 ^b	0.450±0.004 ^b	0.693±0.010 ^b	1.982±0.046 ^b	0.479±0.012 ^b
NAFLD+AST 组	10	0.873±0.021 ^{bc}	0.816±0.013 ^{bc}	0.882±0.009 ^{bc}	1.645±0.296 ^{bc}	0.808±0.011 ^{bc}
F/P 值		69.549/<0.001	786.174/<0.001	183.822/<0.001	182.037/<0.001	296.000/<0.001

注:与空白对照组比较,^a $P<0.05$;与 NAFLD 组比较,^b $P<0.05$;与 NAFLD+Erastin 组比较,^c $P<0.05$ 。

氧化应激和炎症反应是推动疾病进展的重要因素,其导致的脂质代谢紊乱在 NAFLD 的发生发展中起着核心作用^[15-17]。本研究发现,AST 能显著改善肝脏的脂质代谢,降低血液中的脂质水平。这一发现与 AST 通过调节脂质代谢相关酶来促进脂质分解代谢的作用一致,并且 SLC7A11 可能通过参与脂质的转运,协同调节脂质的分配和排泄^[18-20]。此外,Erastin 也表现出对脂质指标的调控作用,这可能与 Erastin 对细胞代谢途径的特殊影响有关^[21-22]。氧化应激与炎症反应的密切关系在 NAFLD 的发病过程中得到了广泛关注。本研究发现,NAFLD 组小鼠中 GSH 水平下降、ROS 和 MDA 水平升高,以及 TNF- α 和 IL-6 的上调,这些变化表明氧化应激与炎症反应相互作用,形成恶性循环,促进疾病的进展^[23-24]。AST 的干预通过抑制氧化应激反应,显著改善上述指标,这与文献中 AST 的抗炎和抗氧化作用一致^[25]。

本研究发现,NAFLD 小鼠模型中自噬标志物 LC3B 上调而 p62 下调,表明自噬通路发生了异常激活^[26]。这一变化可能加剧了氧化应激和炎症反应,促进了病理进展。AST 干预能够有效逆转这一变化,调节自噬通路,减轻肝细胞损伤^[27]。这一发现与以往关于自噬在 NAFLD 中的双重作用的研究相吻合,并为进一步探讨自噬、氧化应激与炎症反应在 NAFLD 中的相互作用提供了新的见解^[28]。铁死亡作为一种以铁依赖性脂质过氧化为特征的程序性细胞死亡形式,在 NAFLD 发生发展中的作用已受到广泛关注^[29-30]。在本研究中,SLC7A11 和 GPX4 表达的下降与铁死亡标志物的上升相吻合,提示氧化应激和脂质过氧化可能是铁死亡的诱因^[31]。AST 通过抑制铁死亡,间接改善了自噬通路,显示出其在 NAFLD 治疗中的潜力,这一点与文献中关于铁死亡在肝脏疾病中的作用相一致^[32-33]。本研究进一步提出了铁死亡与自噬之间的相互作用,这一发现可能为 NAFLD 的综合治疗提供新的策略^[34]。

4 结 论

综上所述,本研究明确了 AST 可抑制 NAFLD 模型中铁死亡和自噬异常激活,其机制可能通过上调 SLC7A11 表达实现,为进一步探索 AST 和 SLC7A11 联合治疗 NAFLD 提供了理论基础。然而,本研究仍有部分问题有待进一步研究,如 AST 与 SLC7A11 之间的详细分子交互作用机制尚未完全阐明,其在细胞内可能通过何种信号转导通路相互影响仍需深入探索。此外,本研究主要基于动物模型,其结果在人体中的转化应用潜力还需要详实的临床研究来验证。未来的研究

将进一步聚焦于这些关键问题,以期为 NAFLD 的临床治疗带来新的突破。

利益冲突:所有作者声明无利益冲突

作者贡献声明

柯月、纪文静:设计研究方案,实施研究过程,论文撰写;梁灿灿、王海昆、崔旻:收集资料,分析实验数据,论文修改;姚萍:课题设计,论文修改、审核

参考文献

- [1] Lou TW, Yang RX, Fan JG. The global burden of fatty liver disease: The major impact of China [J]. *Hepatobiliary Surg Nutr*, 2024, 13 (1): 119-123. DOI: 10.21037/hbsn-23-556.
- [2] Targher G, Tilg H, Byrne CD. Non-alcoholic fatty liver disease: A multisystem disease requiring a multidisciplinary and holistic approach [J]. *Lancet Gastroenterol Hepatol*, 2021, 6(7): 578-588. DOI: 10.1016/S2468-1253(21)00020-0.
- [3] Abdelmalek MF. Nonalcoholic fatty liver disease: Another leap forward [J]. *Nat Rev Gastroenterol Hepatol*, 2021, 18(2): 85-86. DOI: 10.1038/s41575-020-00406-0.
- [4] Lv T, Fan X, He C, et al. SLC7A11-ROS/alphaKG-AMPK axis regulates liver inflammation through mitophagy and impairs liver fibrosis and NASH progression [J]. *Redox Biol*, 2024, 72: 103159. DOI: 10.1016/j.redox.2024.103159.
- [5] Kohandel Z, Farkhondeh T, Aschner M, et al. Anti-inflammatory action of astaxanthin and its use in the treatment of various diseases [J]. *Biomed Pharmacother*, 2022, 145: 112179. DOI: 10.1016/j.biopha.2021.112179.
- [6] Chang MX, Xiong F. Astaxanthin and its effects in inflammatory responses and inflammation-associated diseases: Recent advances and future directions [J]. *Molecules*, 2020, 25(22): 5342. DOI: 10.3390/molecules25225342.
- [7] Yu Q, Song L. Unveiling the role of ferroptosis in the progression from NAFLD to NASH: Recent advances in mechanistic understanding [J]. *Front Endocrinol (Lausanne)*, 2024, 15: 1431652. DOI: 10.3389/fendo.2024.1431652.
- [8] Shen Q, Yang M, Wang S, et al. The pivotal role of dysregulated autophagy in the progression of non-alcoholic fatty liver disease [J]. *Front Endocrinol (Lausanne)*, 2024, 15: 1374644. DOI: 10.3389/fendo.2024.1374644.
- [9] Han JH, Ju JH, Lee YS, et al. Astaxanthin alleviated ethanol-induced liver injury by inhibition of oxidative stress and inflammatory responses via blocking of STAT3 activity [J]. *Sci Rep*, 2018, 8(1): 14090. DOI: 10.1038/s41598-018-32497-w.
- [10] Maschalidi S, Mehrotra P, Keceli BN, et al. Targeting SLC7A11 improves efferocytosis by dendritic cells and wound healing in diabetes [J]. *Nature*, 2022, 606(7915): 776-784. DOI: 10.1038/s41586-022-04754-6.
- [11] Wu H, Li N, Peng S, et al. Maresin1 improves hippocampal neuroinflammation and cognitive function in septic rats by activating the SLC7A11 / GPX4 ferroptosis signaling pathway [J]. *Int Immunopharmacol*, 2024, 131: 111792. DOI: 10.1016/j.intimp.2024.111792.
- [12] Ferreira MJ, Rodrigues TA, Pesosa AG, et al. Glutathione and per-

- oxisome redox homeostasis [J]. *Redox Biol*, 2023, 67: 102917. DOI:10.1016/j.redox.2023.102917.
- [13] Li Y, Liu J, Ye B, et al. Astaxanthin alleviates nonalcoholic fatty liver disease by regulating the intestinal flora and targeting the AMPK/Nrf2 signal axis [J]. *J Agric Food Chem*, 2022, 70(34): 10620-10634. DOI:10.1021/acs.jafc.2c04476.
- [14] 赵磊, 王毅, 刘云卓, 等. 虾青素对脂多糖诱导乌鳢肝脏抗氧化、炎症和糖皮质激素受体蛋白表达的影响[J]. *中国畜牧兽医*, 2023, 50(11): 4776-4782. DOI: 10.16431/j.cnki.1671-7236.2023.11.044.
- [15] Manne V, Handa P, Kowdley KV. Pathophysiology of nonalcoholic fatty liver disease/nonalcoholic steatohepatitis [J]. *Clin Liver Dis*, 2018, 22(1): 23-37. DOI:10.1016/j.cld.2017.08.007.
- [16] Anwar SD, Foster C, Ashraf A. Lipid disorders and metabolic-associated fatty liver disease [J]. *Endocrinol Metab Clin North Am*, 2023, 52(3): 445-457. DOI:10.1016/j.ecl.2023.01.003.
- [17] Badmus OO, Hillhouse SA, Anderson CD, et al. Molecular mechanisms of metabolic associated fatty liver disease (MAFLD): Functional analysis of lipid metabolism pathways [J]. *Clin Sci (Lond)*, 2022, 136(18): 1347-1366. DOI:10.1042/CS20220572.
- [18] Yuan Y, Zhao T, Gao W, et al. Reactive oxygen species derived from NADPH oxidase as signaling molecules regulate fatty acids and astaxanthin accumulation in *Chromochloris zofingiensis* [J]. *Front Microbiol*, 2024, 15: 1387222. DOI:10.3389/fmicb.2024.1387222.
- [19] Rochette L, Dogon G, Rigal E, et al. Lipid peroxidation and iron metabolism: Two corner stones in the homeostasis control of ferroptosis [J]. *Int J Mol Sci*, 2022, 24(1): 449. DOI:10.3390/ijms24010449.
- [20] 宋玮, 张钟艺, 张小波, 等. 茺菀丸调控 p53/SLC7A11 信号通路介导氧化损伤及铁死亡减轻动脉粥样硬化 [J]. *中国中药杂志*, 2024, 49(15): 4118-4127. DOI: 10.19540/j.cnki.cjmm.20240401.401.
- [21] Koppula P, Zhuang L, Gan B. Cystine transporter SLC7A11/xCT in cancer: Ferroptosis, nutrient dependency, and cancer therapy [J]. *Protein Cell*, 2021, 12(8): 599-620. DOI: 10.1007/s13238-020-00789-5.
- [22] Chen H, Tan H, Wan J, et al. PPAR- γ signaling in nonalcoholic fatty liver disease: Pathogenesis and therapeutic targets [J]. *Pharmacol Ther*, 2023, 245: 108391. DOI: 10.1016/j.pharmthera.2023.108391.
- [23] Aljobaily N, Viereckl MJ, Hydock DS, et al. Creatine alleviates doxorubicin-induced liver damage by inhibiting liver fibrosis, inflammation, oxidative stress, and cellular senescence [J]. *Nutrients*, 2021, 13(41): 1-15. DOI:10.3390/nu13010041.
- [24] Li M, He Y, Zhou Z, et al. MicroRNA-223 ameliorates alcoholic liver injury by inhibiting the IL-6-p47 (phox)-oxidative stress pathway in neutrophils [J]. *Gut*, 2017, 66(4): 705-715. DOI:10.1136/gutjnl-2016-311861.
- [25] Wang X, Liu Z, Peng P, et al. Astaxanthin attenuates osteoarthritis progression via inhibiting ferroptosis and regulating mitochondrial function in chondrocytes [J]. *Chem Biol Interact*, 2022, 366: 110148. DOI:10.1016/j.cbi.2022.110148.
- [26] Tanaka S, Hikita H, Tatsumi T, et al. Rubicon inhibits autophagy and accelerates hepatocyte apoptosis and lipid accumulation in nonalcoholic fatty liver disease in mice [J]. *Hepatology*, 2016, 64(6): 1994-2014. DOI:10.1002/hep.28820.
- [27] Liu J, Huang C, Liu J, et al. Nrf2 and its dependent autophagy activation cooperatively counteract ferroptosis to alleviate acute liver injury [J]. *Pharmacol Res*, 2023, 187: 106563. DOI:10.1016/j.phrs.2022.106563.
- [28] Nasiri-Ansari N, Nikolopoulou C, Papoutsi K, et al. Empagliflozin attenuates non-alcoholic fatty liver disease (NAFLD) in high fat diet fed ApoE(-/-) mice by activating autophagy and reducing ER stress and apoptosis [J]. *Int J Mol Sci*, 2021, 22(2): 818. DOI:10.3390/ijms22020818.
- [29] Zhao S, Guo Y, Yin X. Lipid Peroxidation in ferroptosis and association with nonalcoholic fatty liver disease [J]. *Front Biosci (Landmark Ed)*, 2023, 28(12): 332. DOI:10.31083/j.fbl2812332.
- [30] 刘鸣昊, 刘素彤, 张丽慧, 等. 铁死亡的发生机制及其在非酒精性脂肪性肝病/非酒精性脂肪性肝发生发展中的作用 [J]. *临床肝胆病杂志*, 2022, 38(5): 1152-1155. DOI: 10.3969/j.issn.1001-5256.2022.05.037.
- [31] Ursini F, Maiorino M. Lipid peroxidation and ferroptosis: The role of GSH and GPx4 [J]. *Free Radic Biol Med*, 2020, 152: 175-185. DOI: 10.1016/j.freeradbiomed.2020.02.027.
- [32] Park E, Chung SW. Ros-mediated autophagy increases intracellular iron levels and ferroptosis by ferritin and transferrin receptor regulation [J]. *Cell Death Dis*, 2019, 10(11): 822. DOI:10.1038/s41419-019-2064-5.
- [33] 骆倩, 罗涛, 宋针珍, 等. 基于 Nrf2/SLC7A11/GPX4 通路探讨葛根苓连汤通过抑制铁死亡改善非酒精性脂肪性肝病作用机制 [J]. *中国比较医学杂志*, 2025, 35(1): 1-13. DOI: 10.3969/j.issn.1671-7856.2025.01.
- [34] Honma K, Kirihara S, Nakayama H, et al. Selective autophagy associated with iron overload aggravates non-alcoholic steatohepatitis via ferroptosis [J]. *Exp Biol Med (Maywood)*, 2023, 248(13): 1112-1123. DOI:10.1177/15353702231191197.

(收稿日期:2024-12-27)